Supporting Information

Chiral Transcription to Cationic Polycobaltocenes over Multiple Length Scales using Anionic Surfactants

Rebecca A. Musgrave,[1] Paul Choi,[1] Robert L. Harniman,[1] Robert M. Richardson,[2] Chengshuo Shen,[3] George R. Whittell,[1] Jeanne Crassous,[4] Huibin Qiu[3,*] and Ian Manners[1,*]

[1]School of Chemistry and [2]School of Physics, University of Bristol, Bristol, BS8 1TS, United Kingdom.
[3]School of Chemistry and Chemical Engineering, Shanghai Jiao Tong University, Shanghai 200240, China.
[4]Institut des Sciences Chimiques de Rennes UMR 6226, CNRS Université de Rennes 1, Campus de Beaulieu, 35042 Rennes Cedex, France.

*To whom correspondence should be addressed,
E-mail: ian.manners@bristol.ac.uk, hbqiu@sjtu.edu.cn.

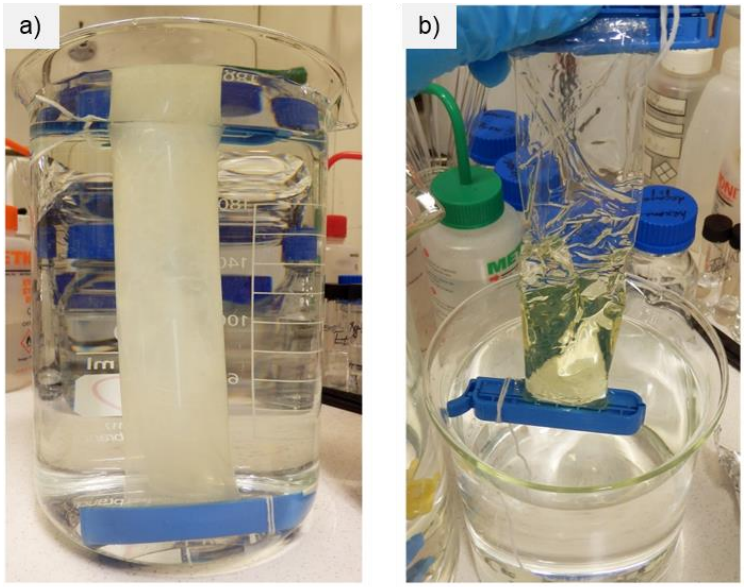

Figure S1. Representative photographs of the $[PCE][A^*]_n$ complexes during dialysis against water and ethanol: a) the $[PCE][A^*]_n$ complexes are insoluble in water and formed a precipitate during dialysis against water b) on further dialysis against ethanol, the precipitate gradually dissolves, and a clear yellow solution eventually formed.

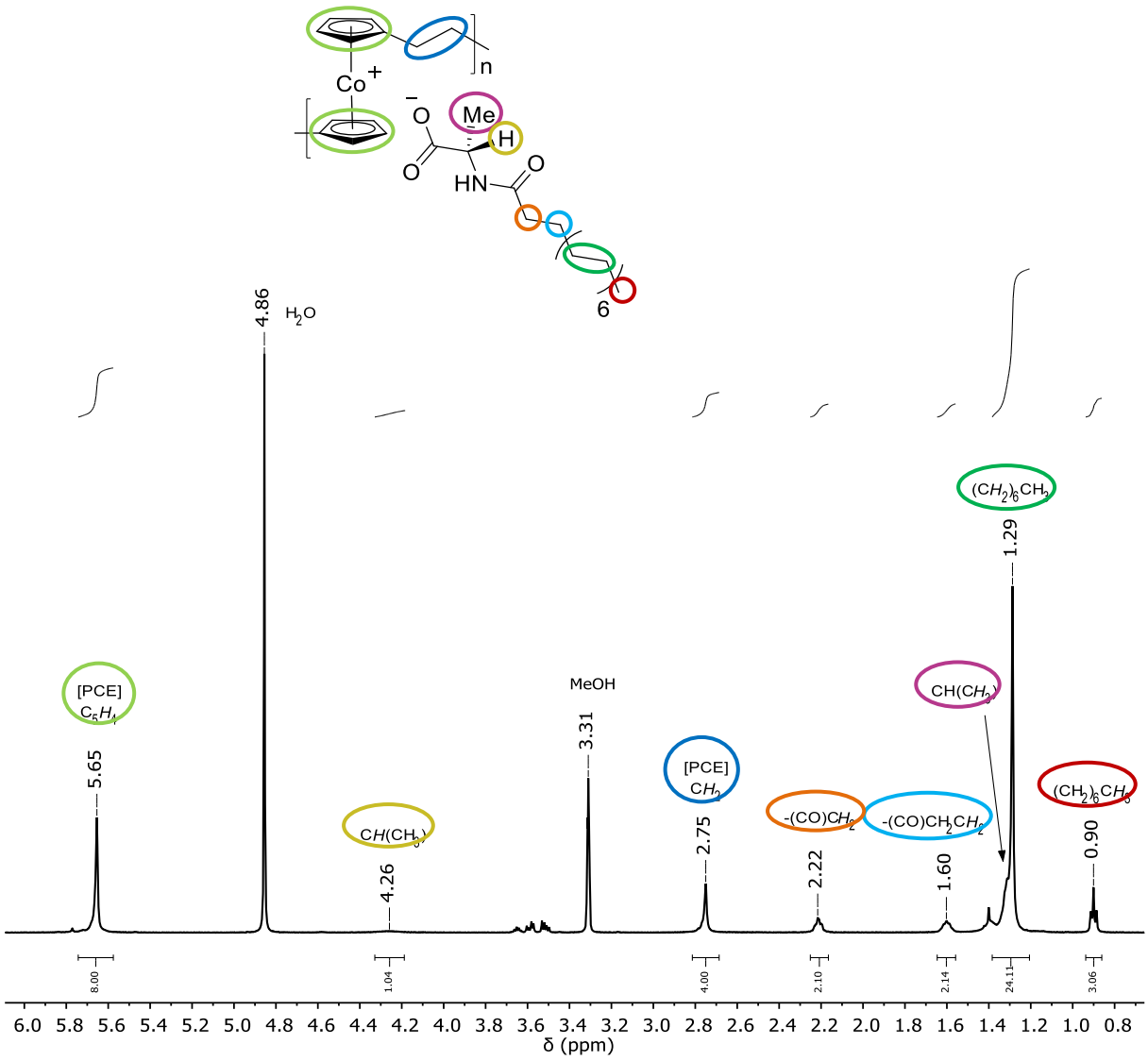

Figure S2. ^{1}H NMR (500 MHz, CD_3OD) spectrum of [PCE][C_{16}-L-Ala]$_n$ complex.

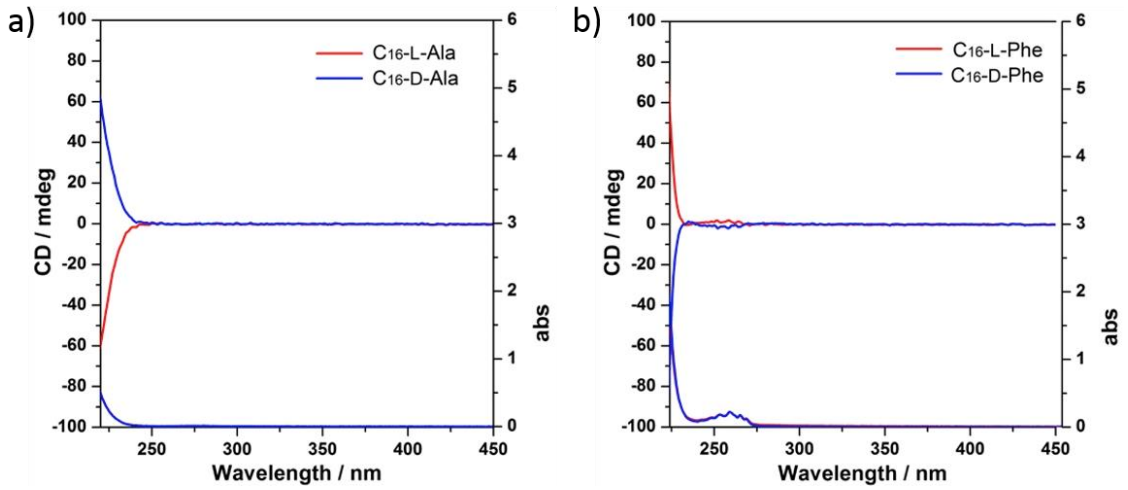

Figure S3. CD and UV-vis spectra of aqueous solutions of a) [Na][C_{16}-L-Ala] and [Na][C_{16}-D-Ala], and b) [Na][C_{16}-L-Phe] and [Na][C_{16}-D-Phe], all at 0.5 mg mL^{-1} in EtOH.

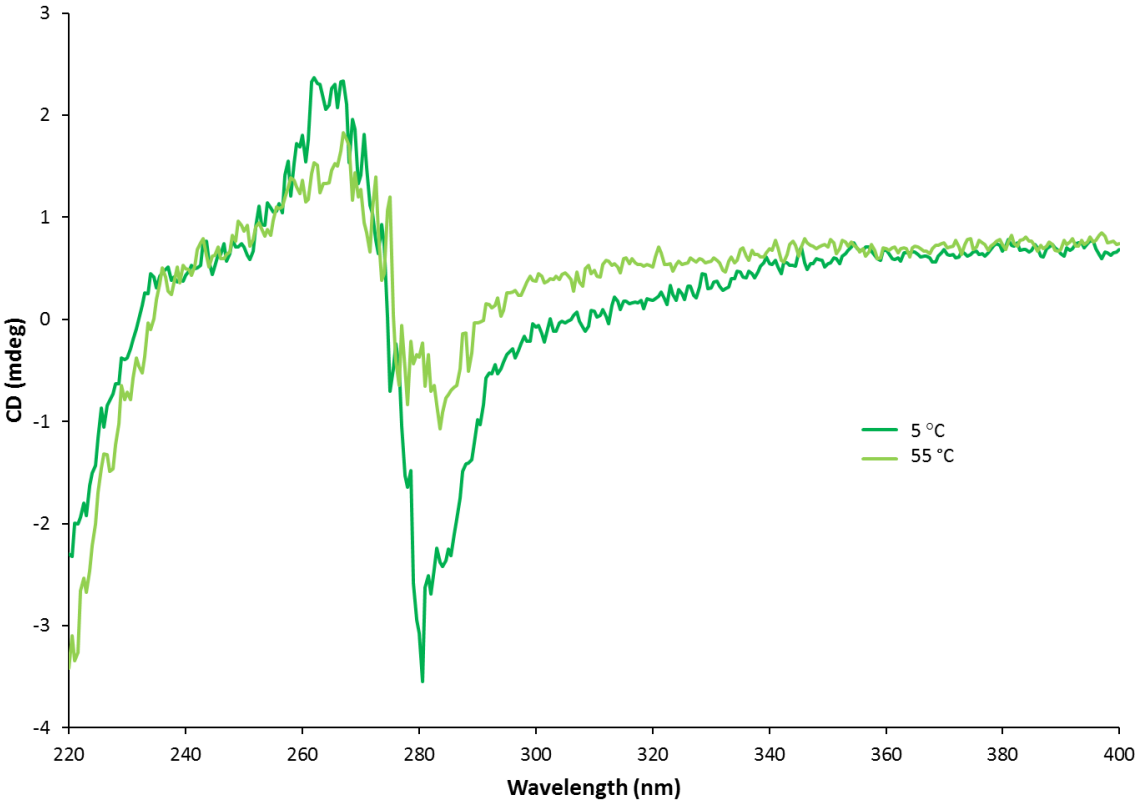

Figure S4. CD spectra of [PCE][C_{16}-L-Ala]$_n$ at 0.5 mg mL^{-1} in EtOH taken at 5 °C and 55 °C.

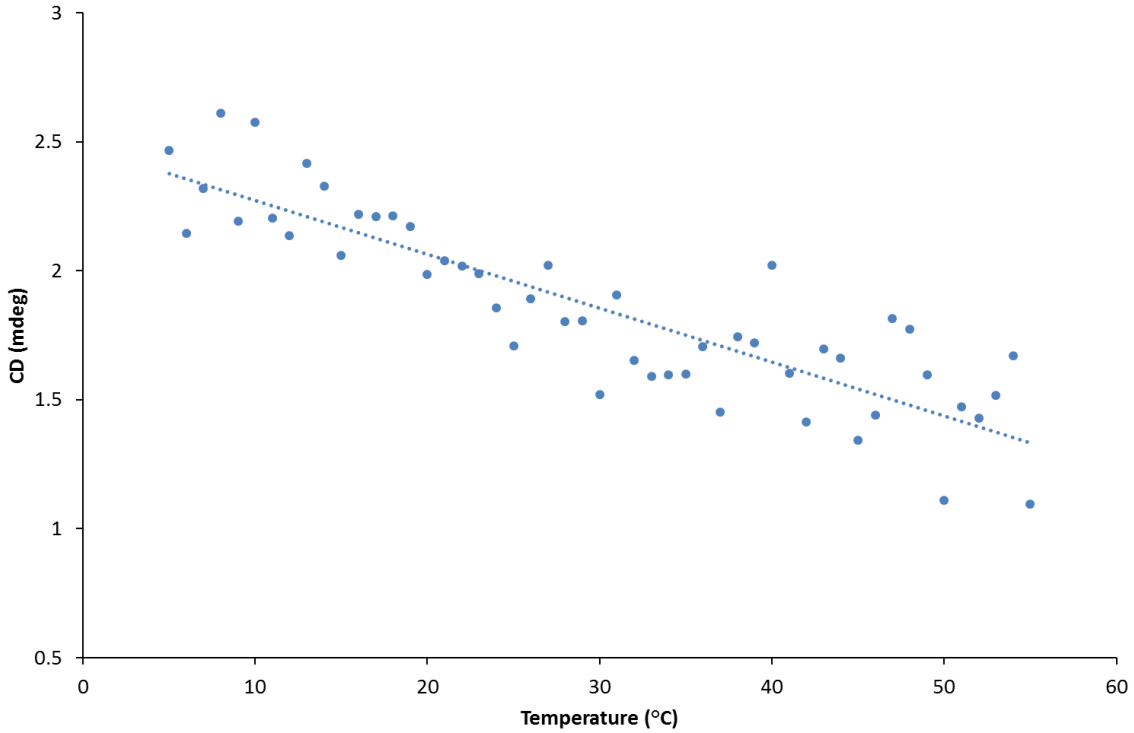

Figure S5. CD response of [PCE][C_{16}-L-Ala]$_n$ at 0.5 mg mL^{-1} in EtOH at 266 nm over a range of temperatures (5 °C to 55 °C).

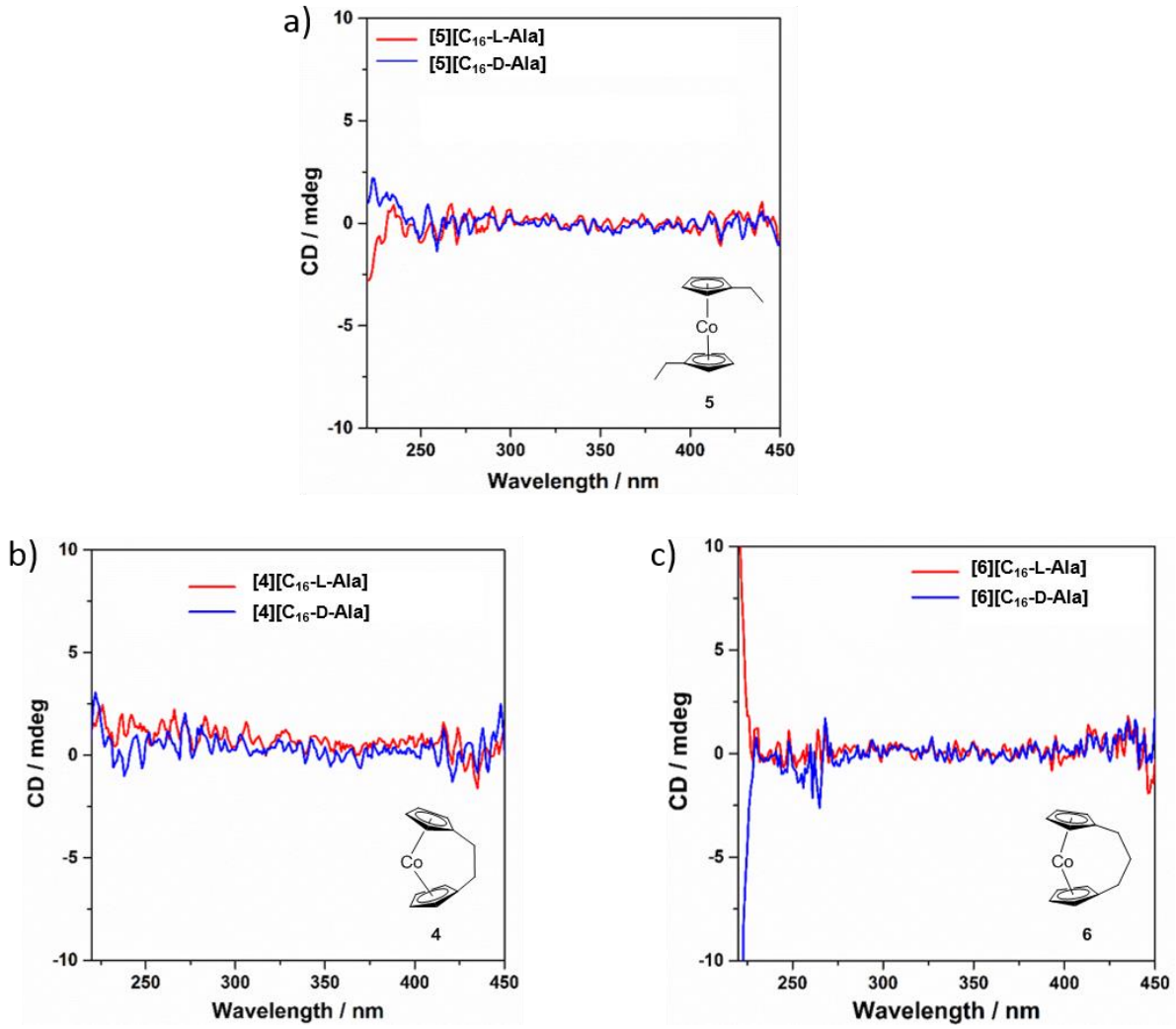

Figure S6. CD spectra of complexes formed by (a) bis(ethylcyclopentadienyl) cobalt(III), (b) dicarba[2]cobaltocenophanium and (c) tricarba[3]cobaltocenophanium with $[C_{16}\text{-L-Ala}]^-$ (red lines) and $[C_{16}\text{-D-Ala}]^-$ (blue line), all at 0.5 mg mL^{-1} in EtOH.

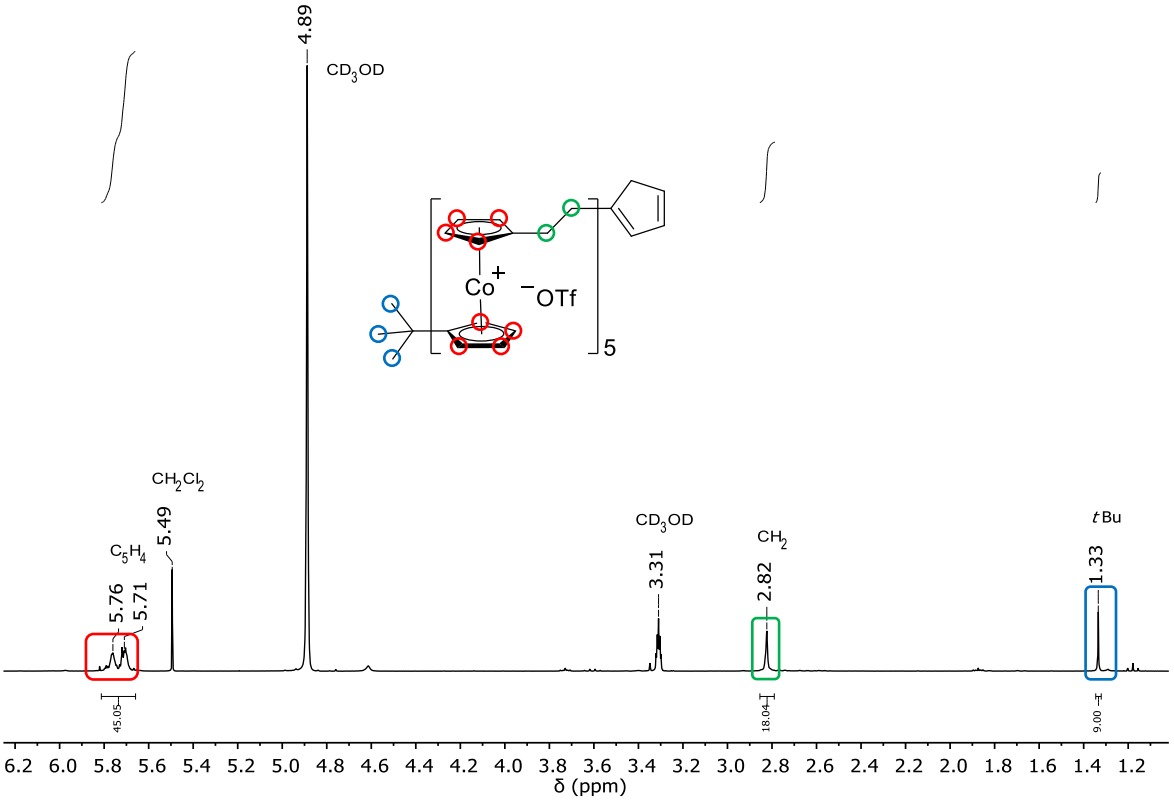

Figure S7. ^{1}H NMR (300 MHz, CD_3OD) spectrum of $[OCE_5][OTf]_5$ complex.

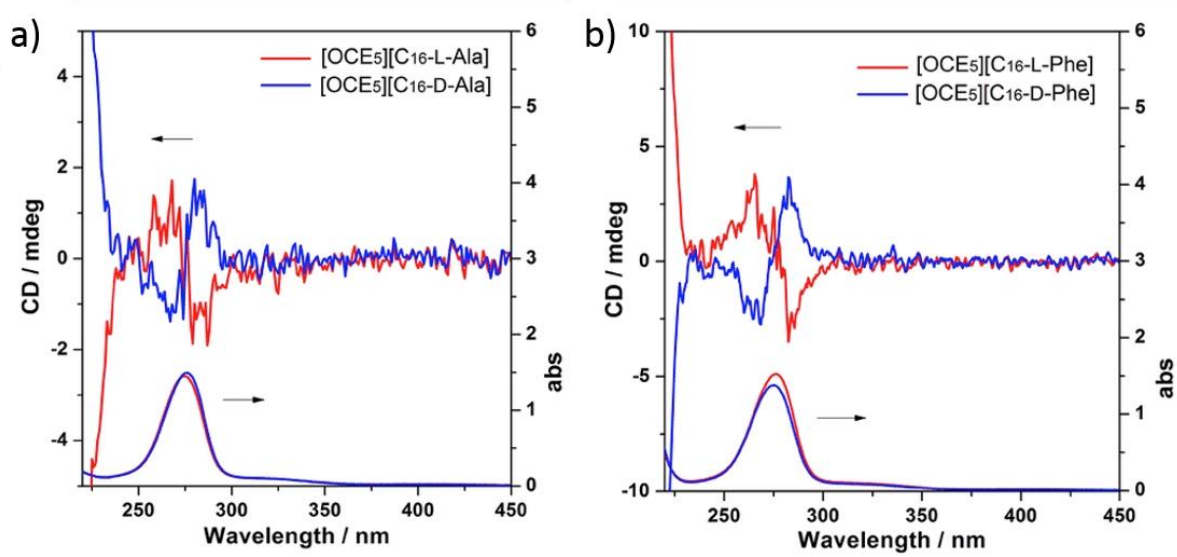

Figure S8. CD and UV-vis spectra of solutions of a) $[OCE_5][C_{16}$-L-Ala$]_5$ and $[OCE_5][C_{16}$-D-Ala$]_5$ complexes and b) $[OCE_5][C_{16}$-L-Phe$]_5$ and $[OCE_5][C_{16}$-D-Phe$]_5$ complexes, all at 0.5 mg mL^{-1} in EtOH.

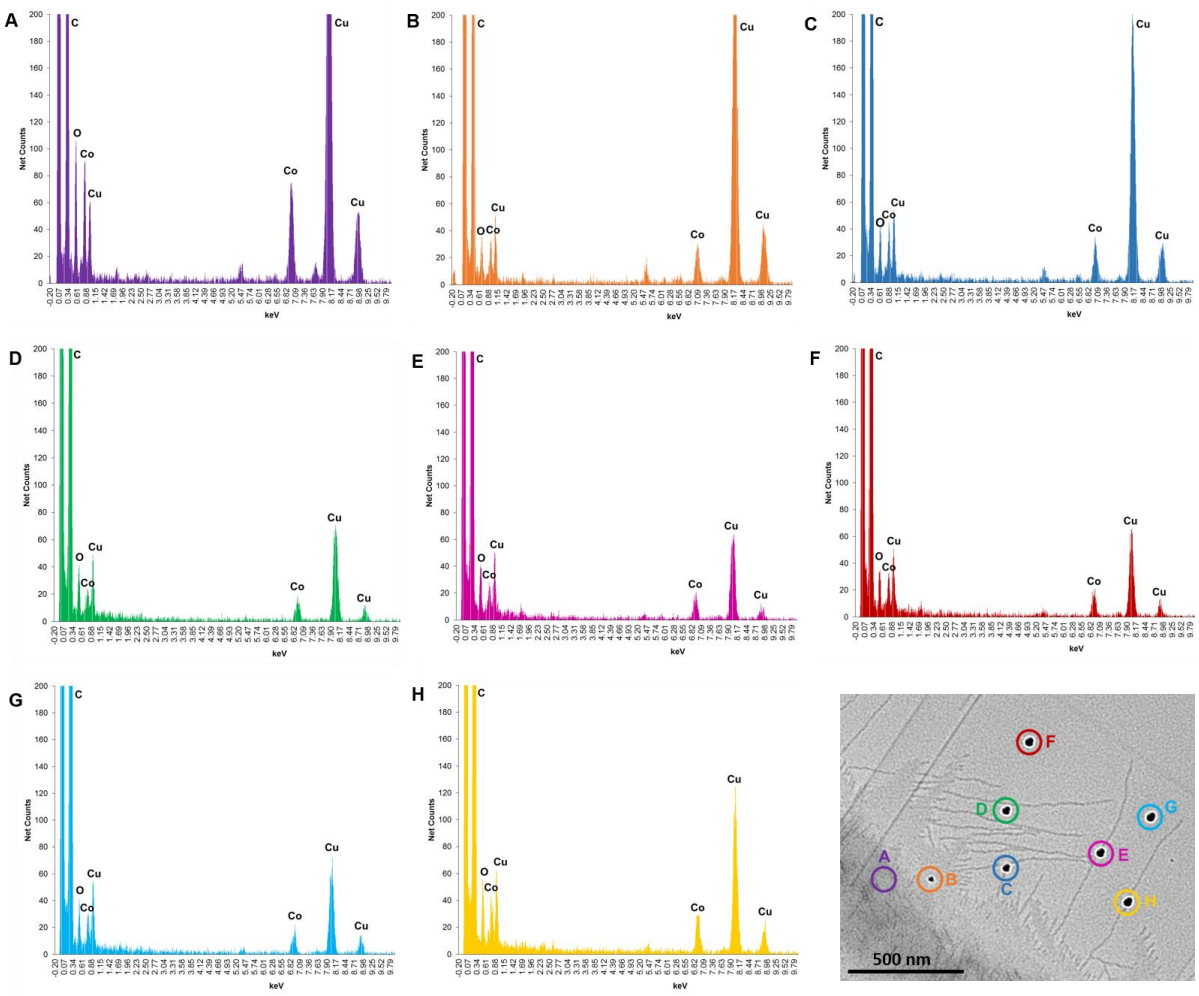

Figure S9. EDX analyses of spots A, B, C, D, E, F, G and H of [PCE][C_{16}-L-Ala]$_n$ solution in ethanol, drop cast onto a carbon-coated copper TEM grid. The detection of Cu in all cases is due to the use of copper TEM grids.

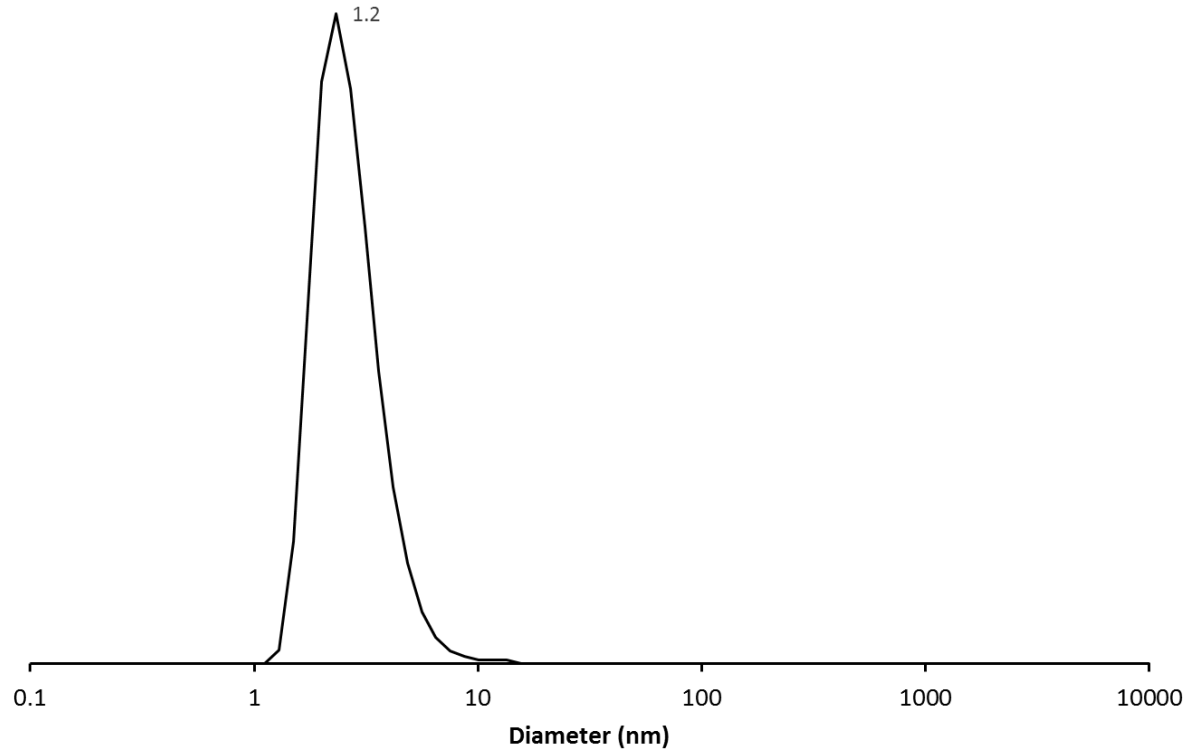

Figure S10. DLS size distribution by volume of [PCE][C_{16}-L-Ala]$_n$ complex (EtOH, 25 °C, 12 mg mL^{-1}). R_h = 1.2 nm.

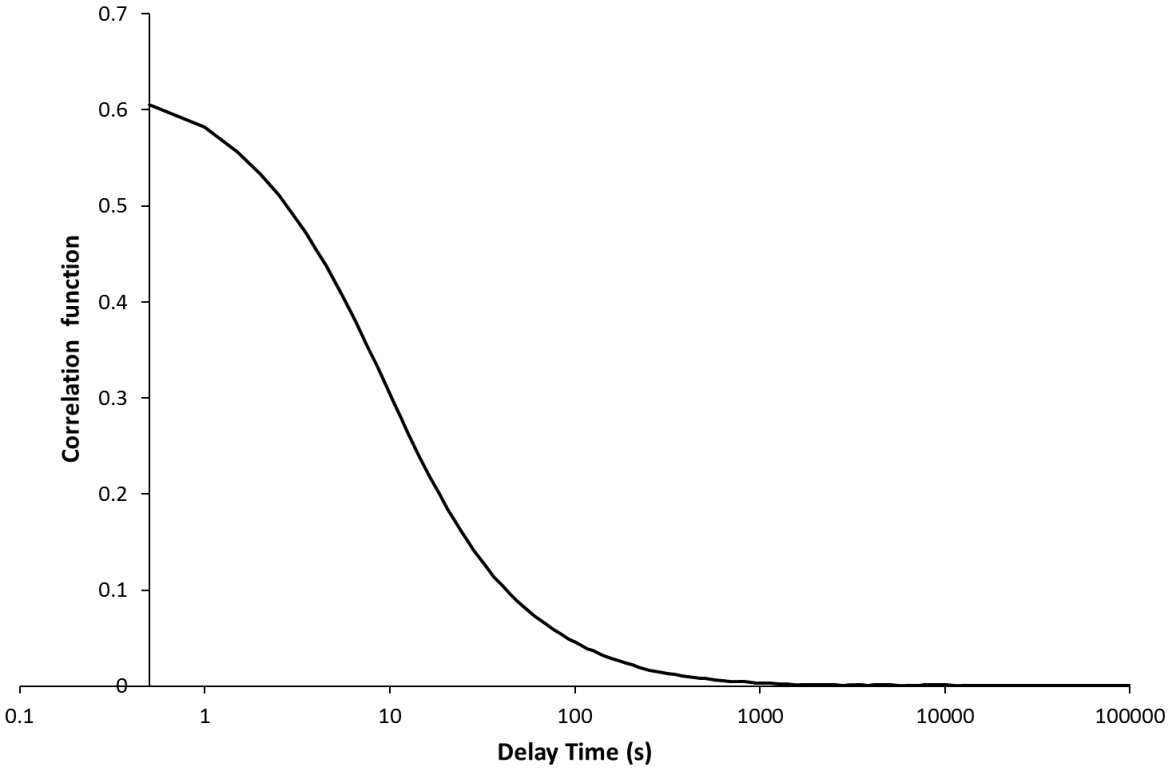

Figure S11. Raw DLS correlation data of [PCE][C_{16}-L-Ala]$_n$ complex (EtOH, 25 °C, 12 mg mL^{-1}).

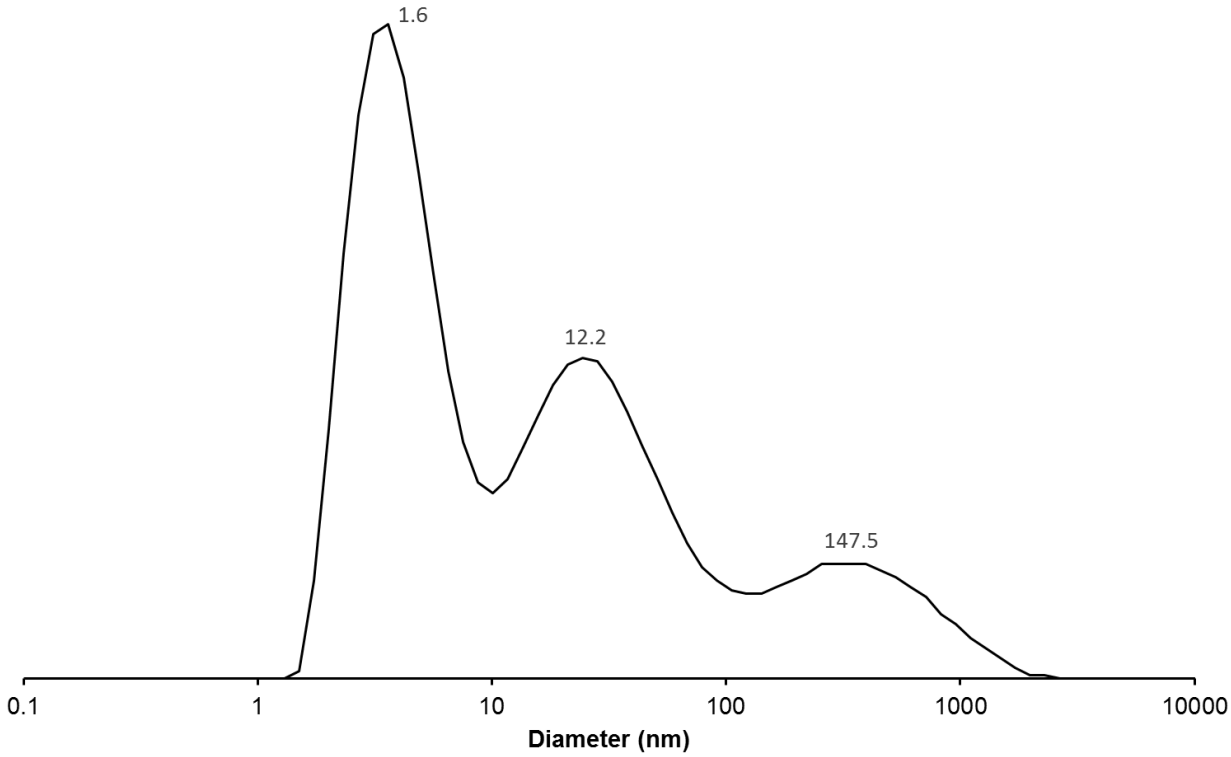

Figure S12. DLS size distribution by intensity of [PCE][C_{16}-L-Ala]$_n$ complex (EtOH, 25 °C, 12 mg mL^{-1}). R_h = 1.6 nm, 12.2 nm, 147.5 nm.

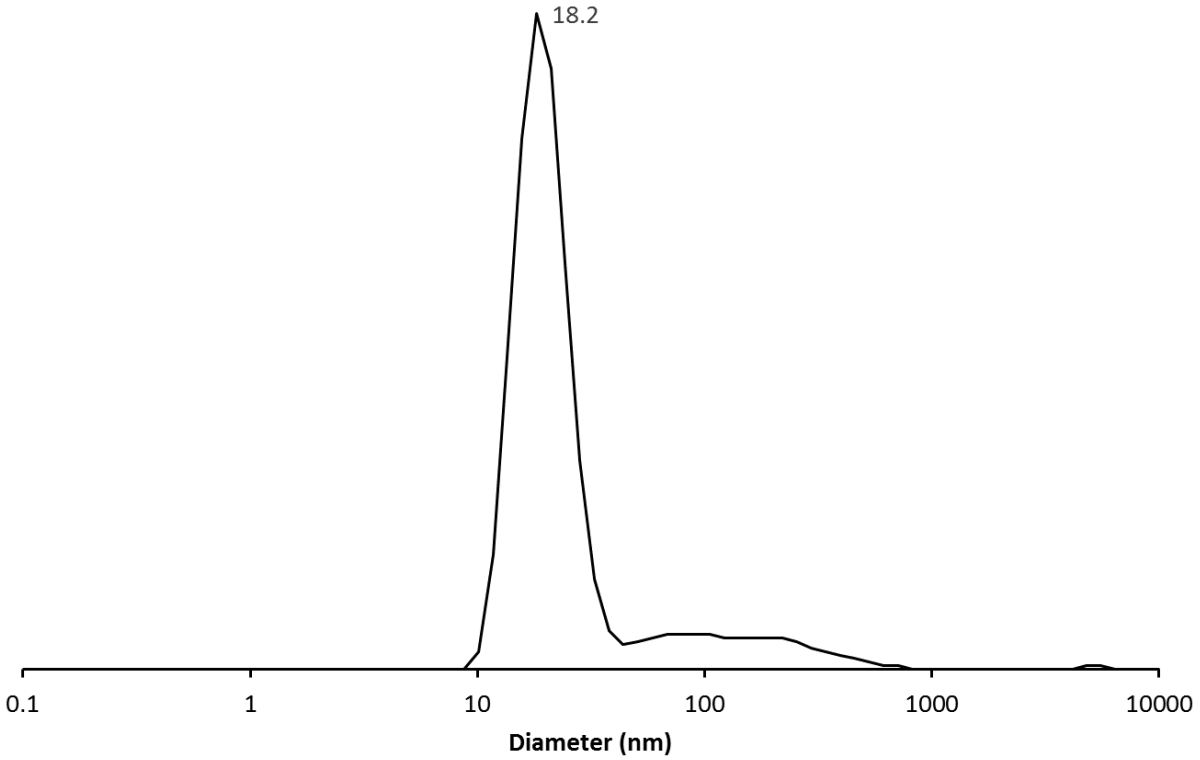

Figure S13. DLS size distribution by volume of [PCE][Cl]$_n$ complex (H_2O, 25 °C, 2 mg mL^{-1}). R_h = 18.2 nm.

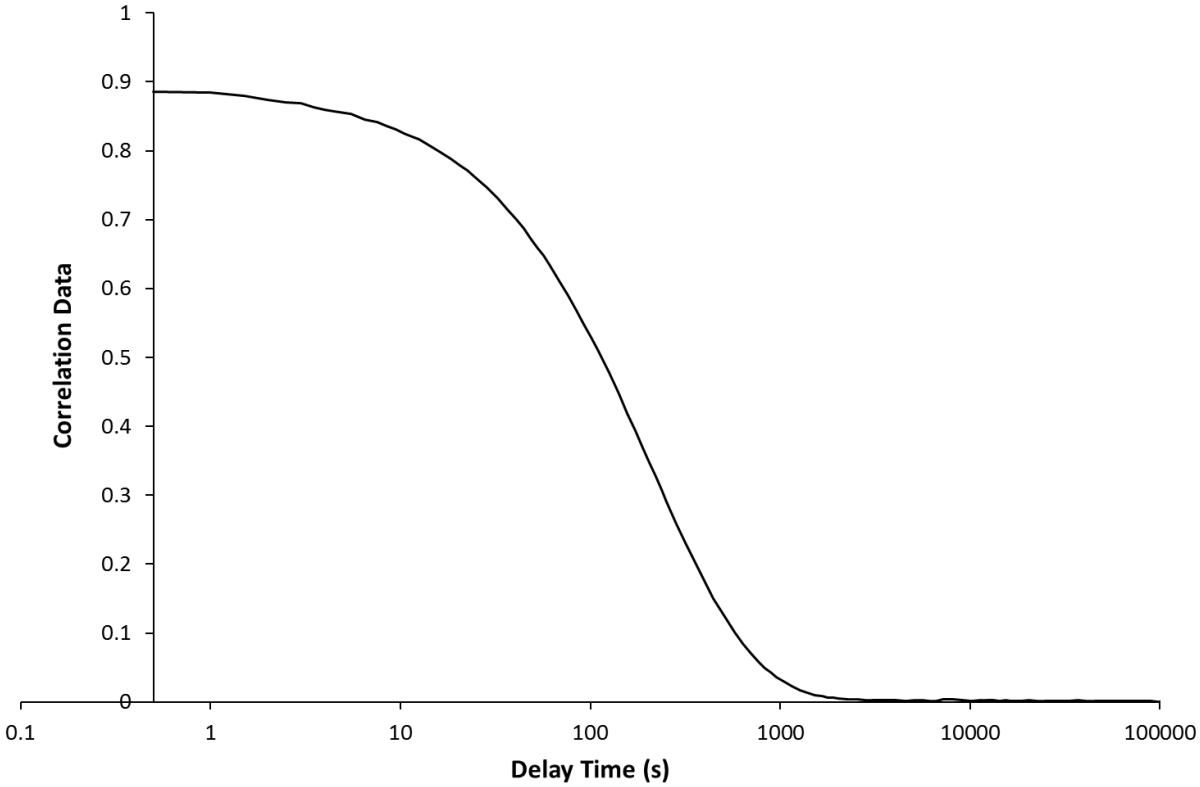

Figure S14. Raw DLS correlation data of $[PCE][Cl]_n$ complex (H_2O, 25 °C, 2 mg mL^{-1}).

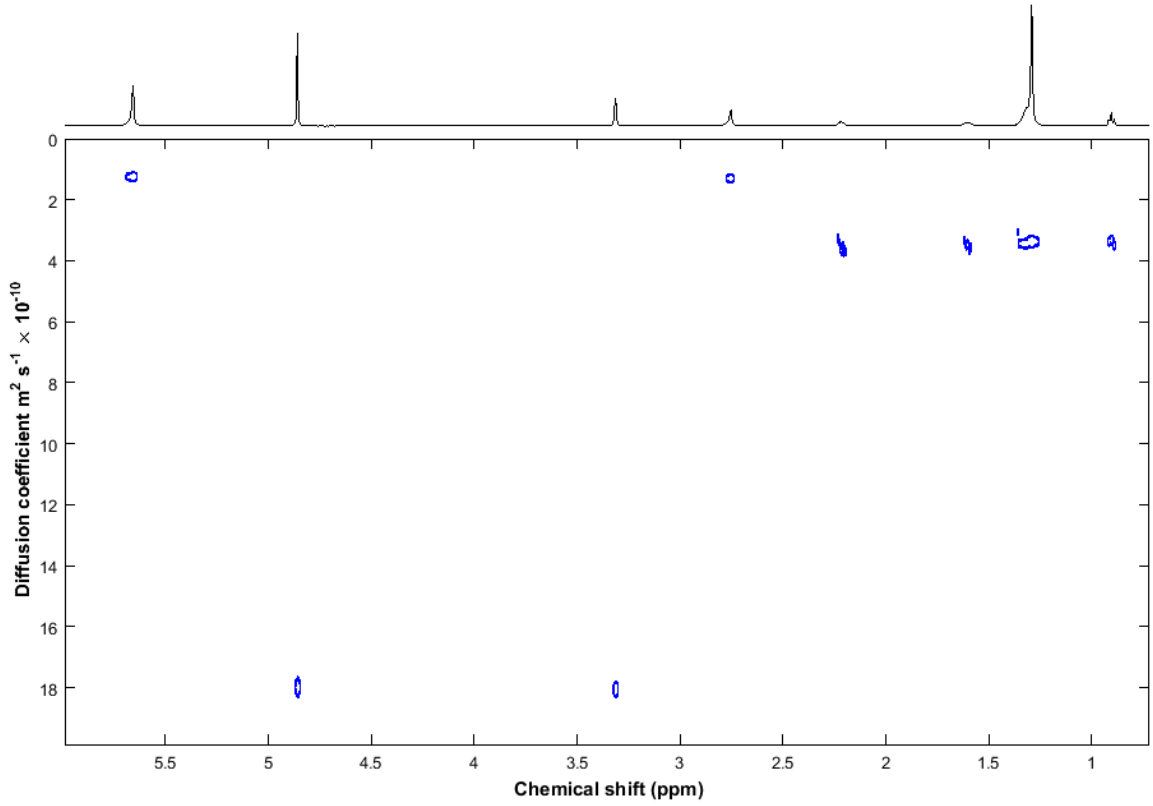

Figure S15. ^1H DOSY NMR (500 MHz, CD_3OD) spectrum of $[PCE][C_{16}$-L-Ala$]_n$ complex.

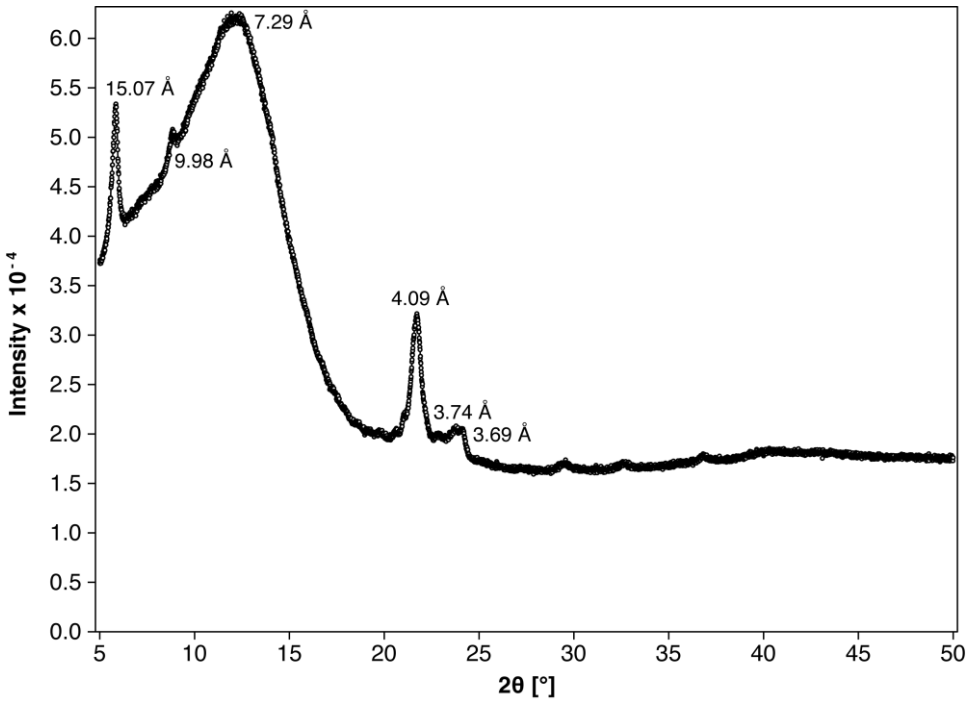

Figure S16. WAXS data for [PCE][C_{16}-L-Ala]$_n$ drop cast from an ethanolic solution (12 mg mL^{-1}).

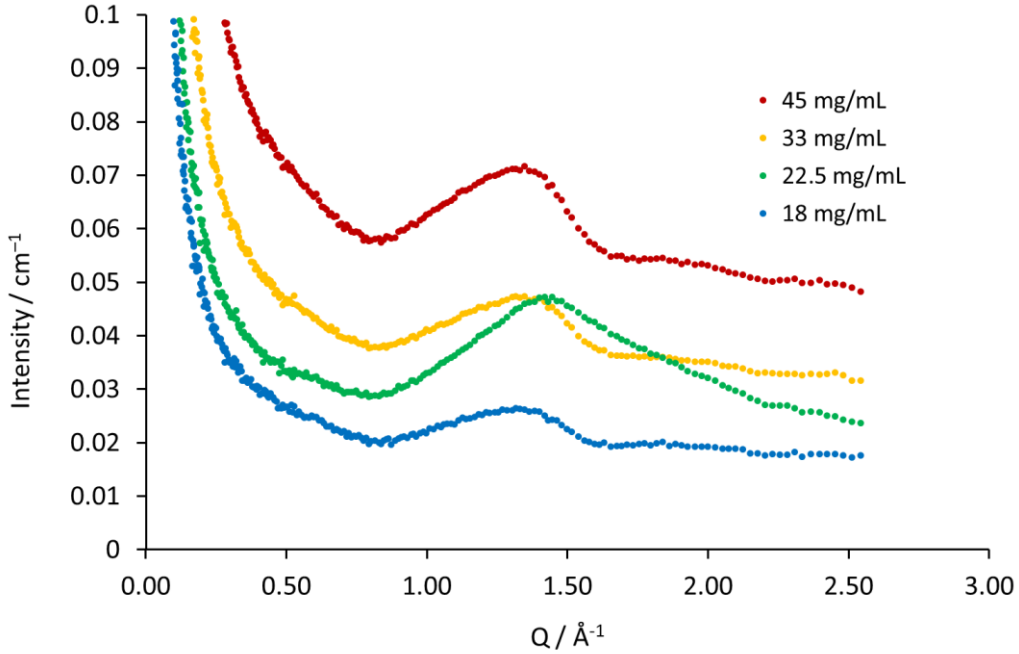

Figure S17. Small angle X-ray scattering data: plot of the scattered intensity (*I*) versus the magnitude of the scattering vector (*Q*) for [PCE][C_{16}-L-Ala]$_n$ at various concentrations in ethanol.

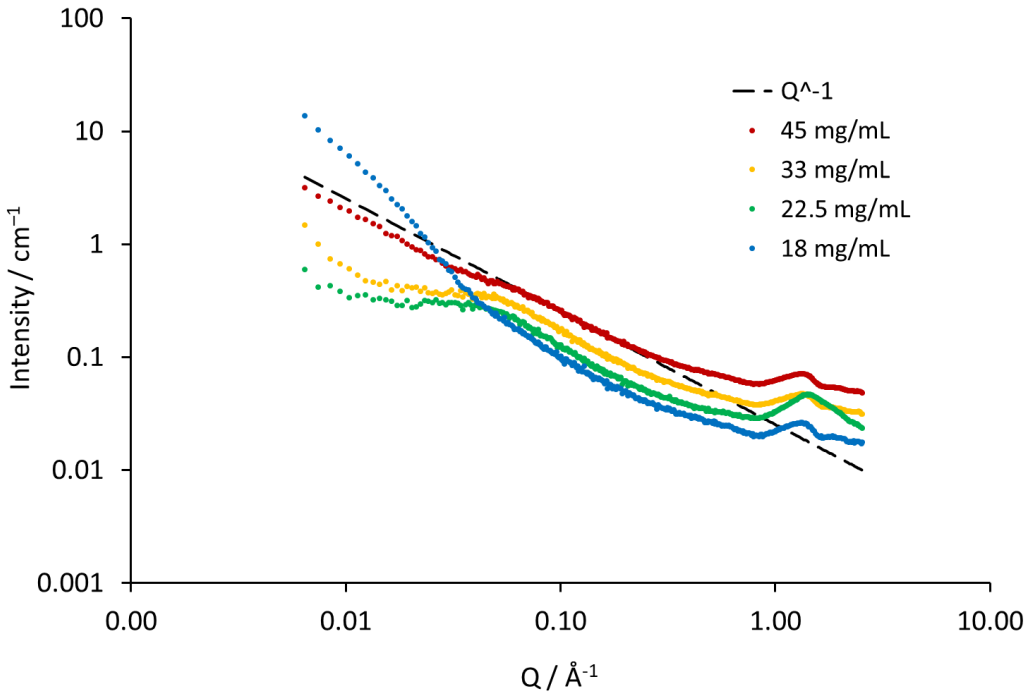

Figure S18. Small angle X-ray scattering data: log-log plot of the scattered intensity (*I*) versus the magnitude of the scattering vector (*Q*) for [PCE][C_{16}-L-Ala]$_n$ at various concentrations in ethanol.

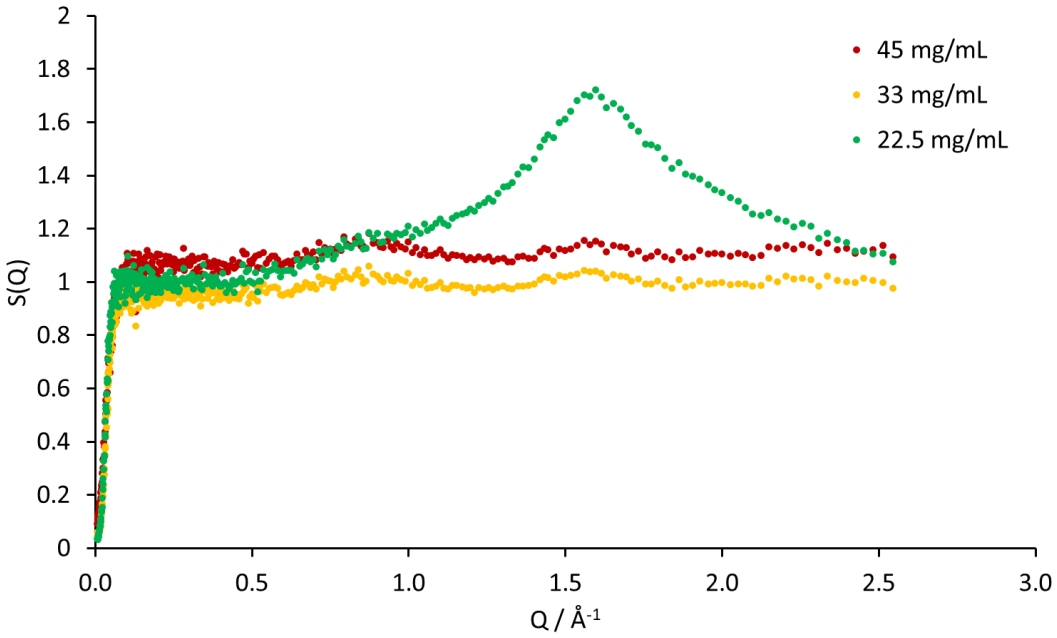

Figure S19. Small angle X-ray scattering data: plot of the product of the scattering factor *S(Q)* versus the magnitude of the scattering vector (*Q*) for [PCE][C_{16}-L-Ala]$_n$ at various concentrations in ethanol.

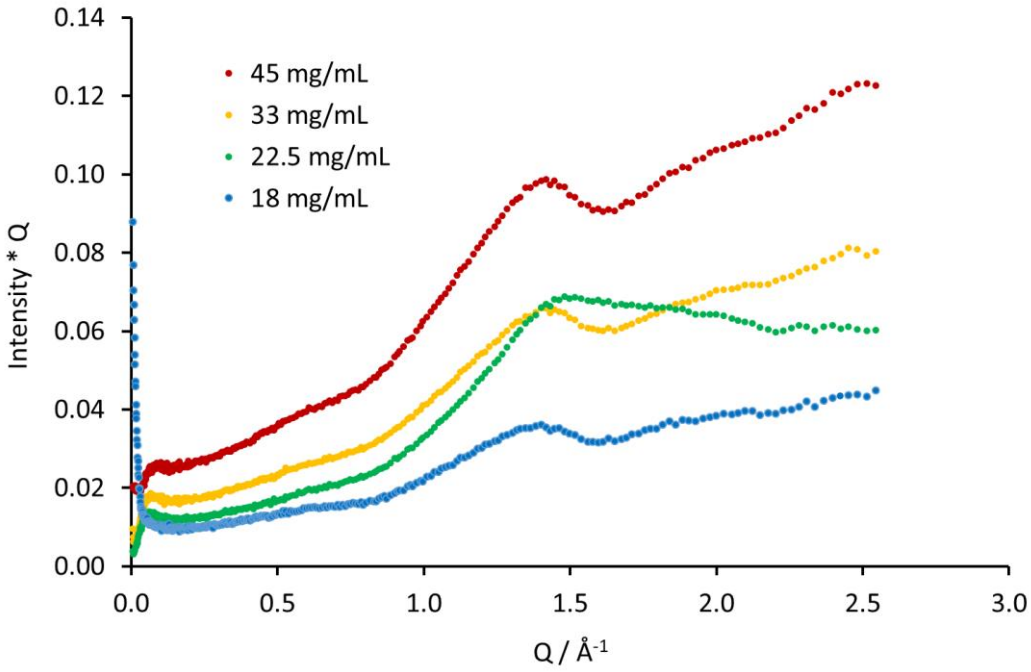

Figure S20. Small angle X-ray scattering data: plot of the product of the scattered intensity and the scattering vector (*I***Q*) versus the magnitude of the scattering vector (*Q*) for [PCE][C_{16}-L-Ala]$_n$ at various concentrations in ethanol.

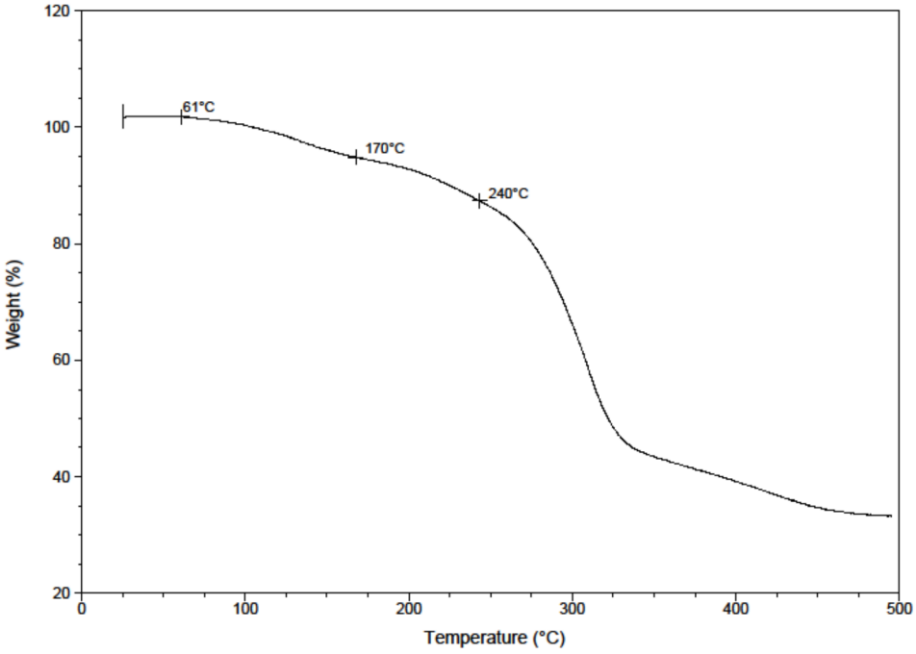

Figure S21. TGA thermogram for [PCE][C_{16}-L-Ala]$_n$ drop cast from an ethanolic solution (12 mg mL^{-1}).

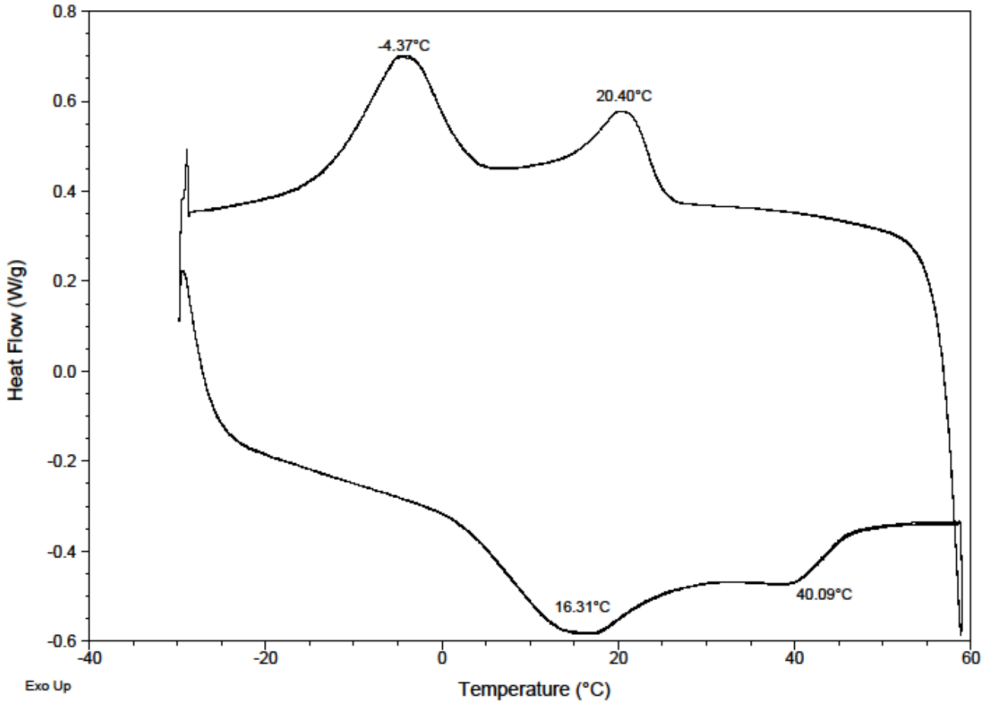

Figure S22. DSC thermogram for [PCE][C_{16}-L-Ala]$_n$ drop cast from an ethanolic solution (12 mg mL^{-1}) obtained at a scan rate of 10 °C min^{-1}.

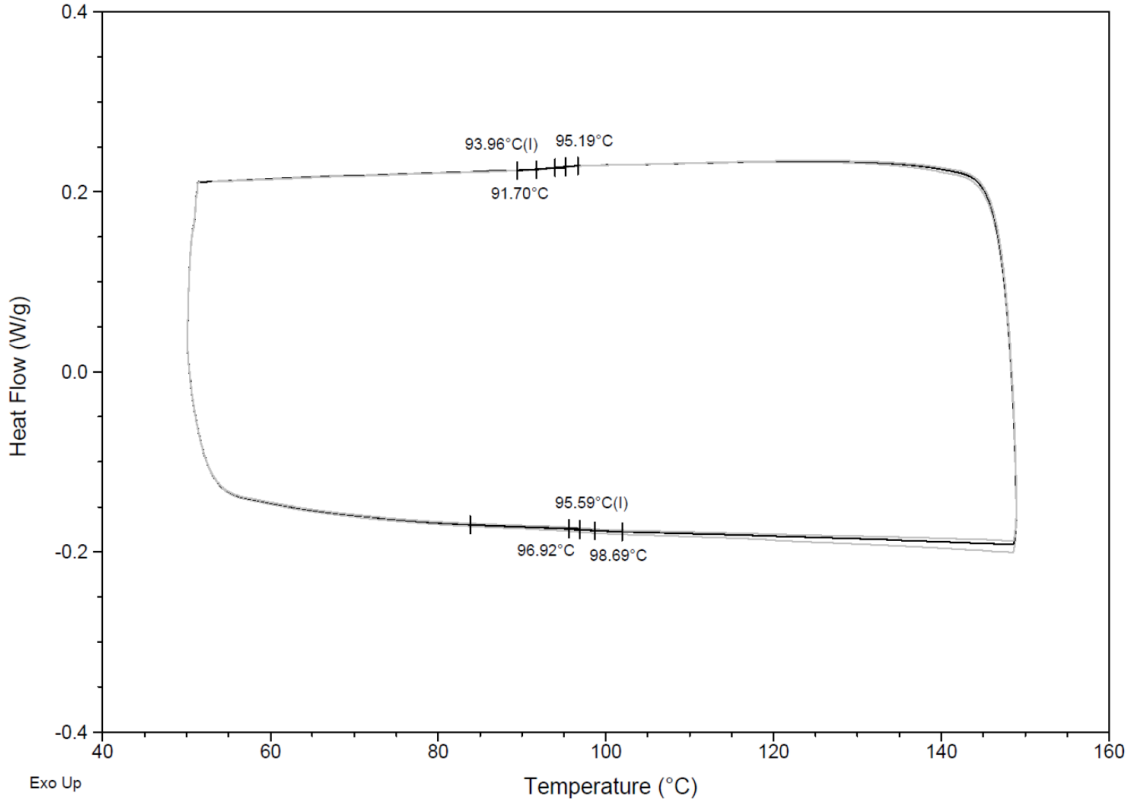

Figure S23. DSC thermogram for [PCE][Cl]$_n$ solid obtained at a scan rate of 10 °C min^{-1}.

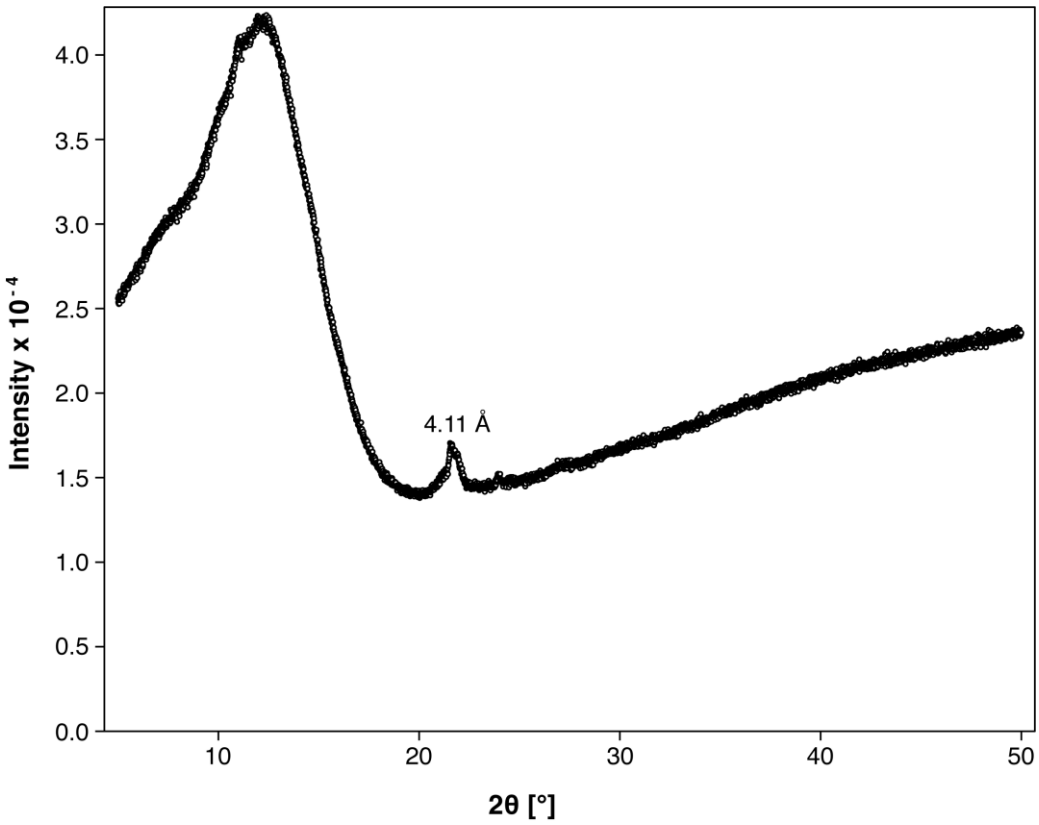

Figure S24. WAXS data for $[PCE][Cl]_n$ solid.

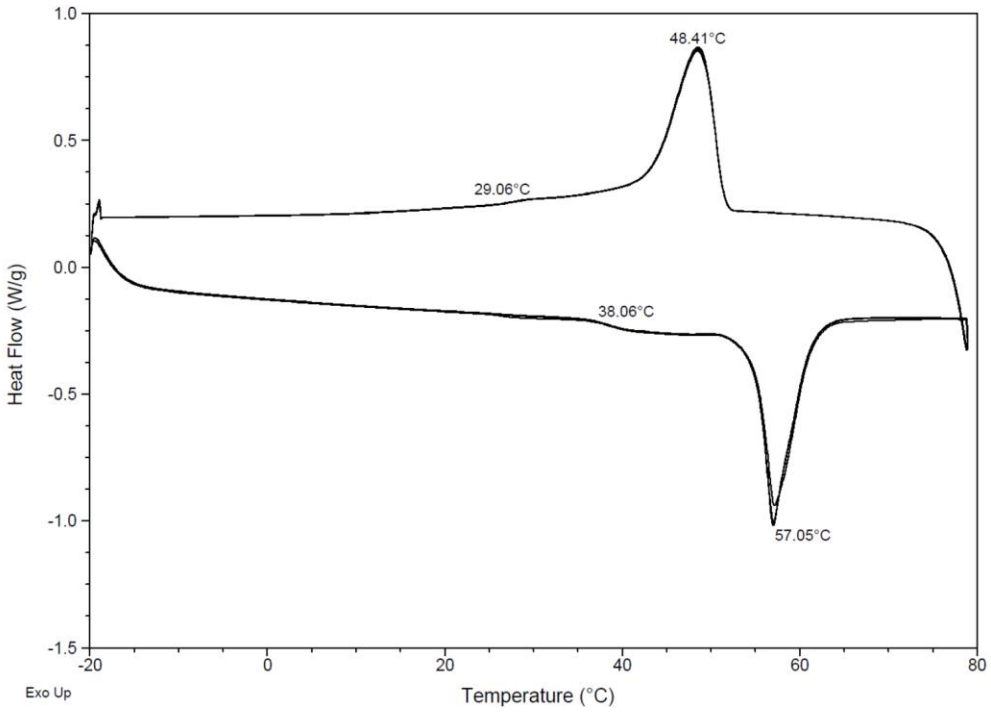

Figure S25. DSC thermogram for $[Na][C_{16}$-L-Ala] (drop cast from a concentrated ethanol solution) obtained at a scan rate of 10 °C min^{-1}.

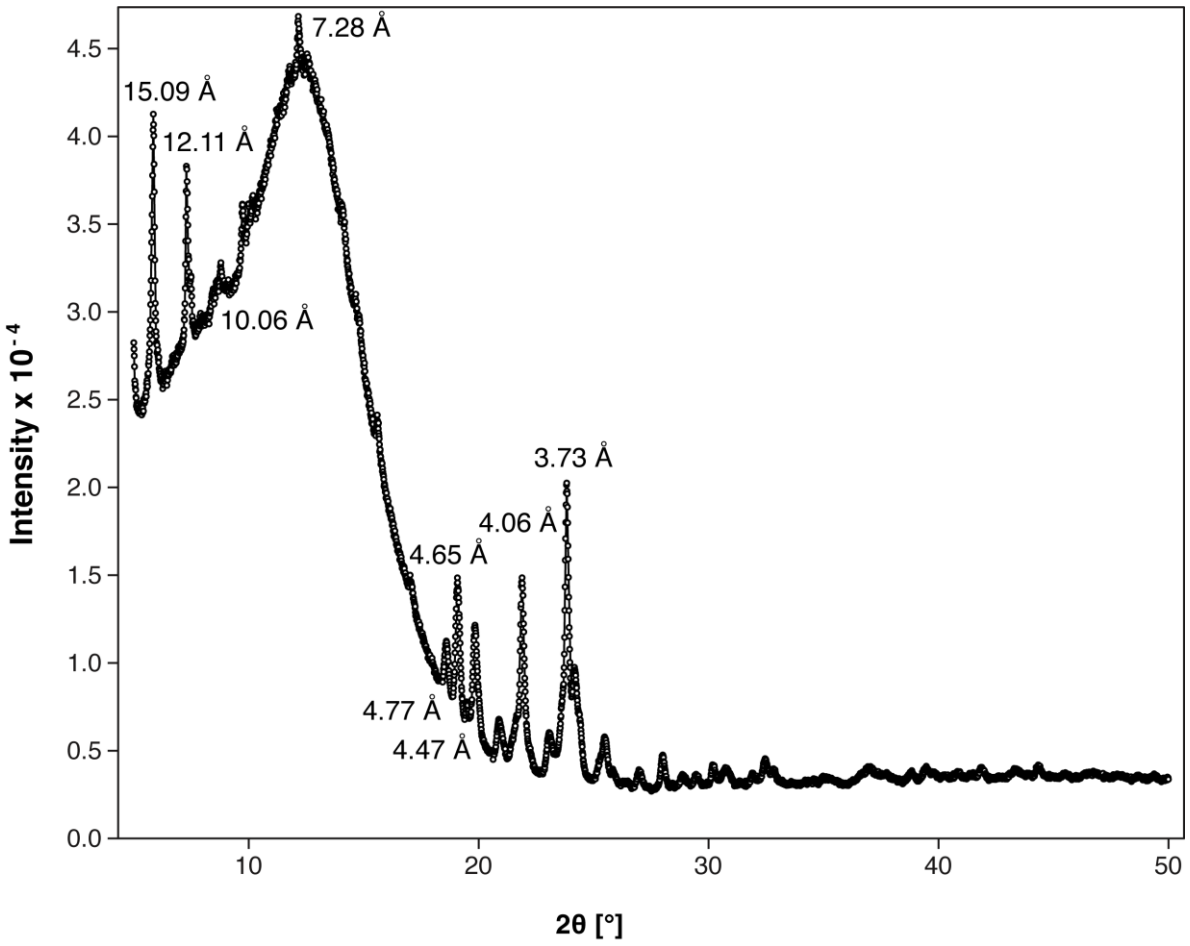

Figure S26. WAXS data for [Na][C_{16}-L-Ala] (drop cast from a concentrated ethanol solution)

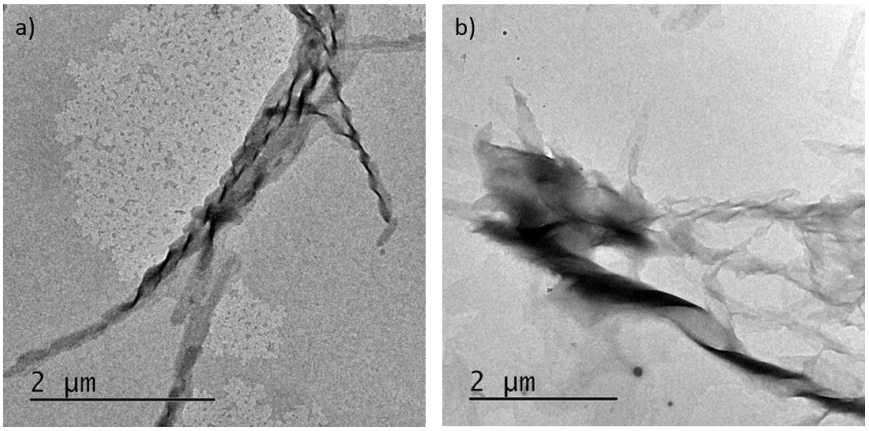

Figure S27. Additional representative TEM images of assemblies of [PCE][C_{16}-L-Ala]$_n$ in water on a carbon-coated copper grid, showing a) tightly twisted helices, and b) a larger twisted coil.

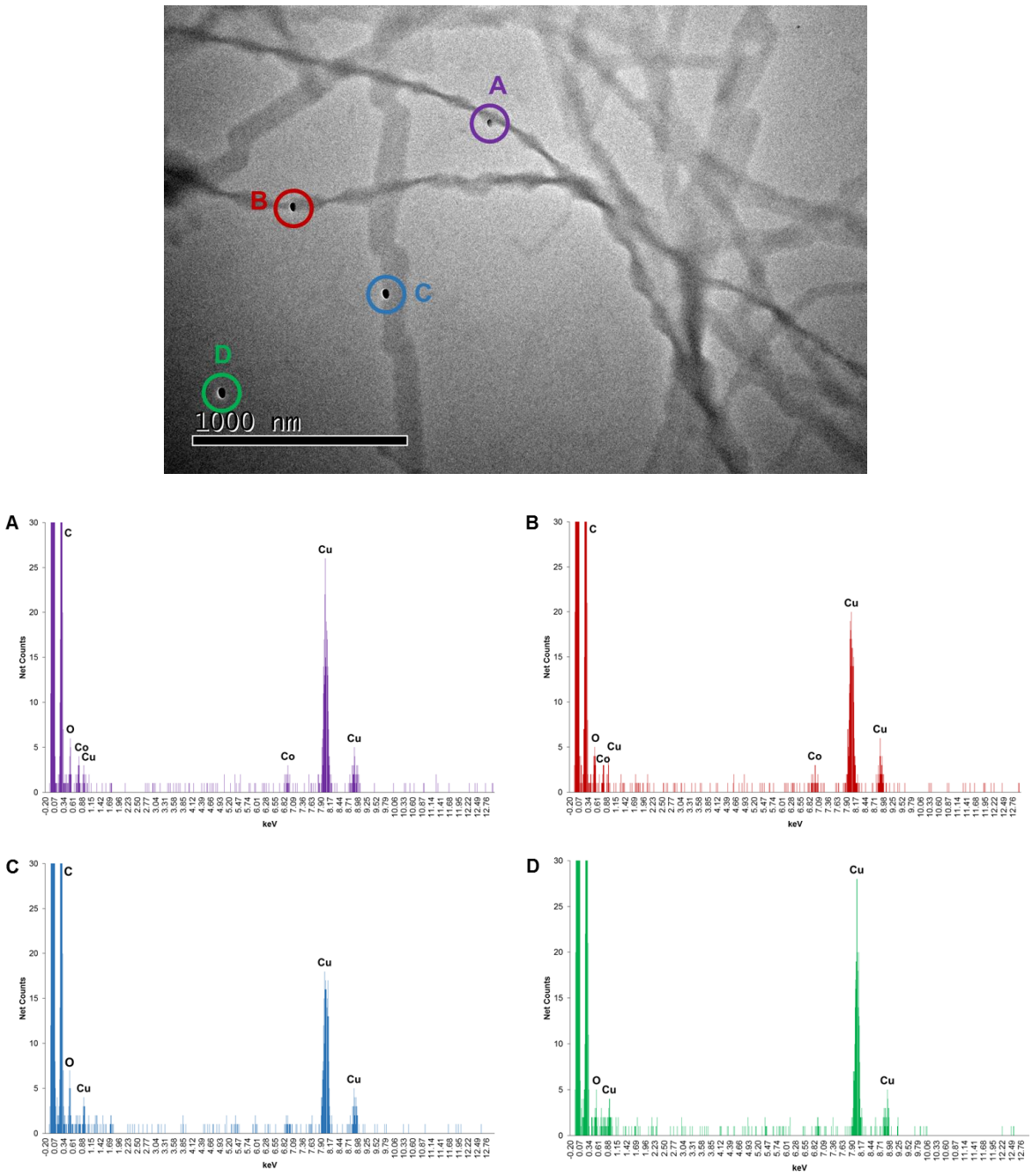

Figure S28. EDX analyses of spots A, B, C and D of [PCE][C_{16}-L-Ala]$_n$ suspension in water, drop cast onto a carbon-coated copper TEM grid. The detection of Cu in all cases is due to the use of copper TEM grids.

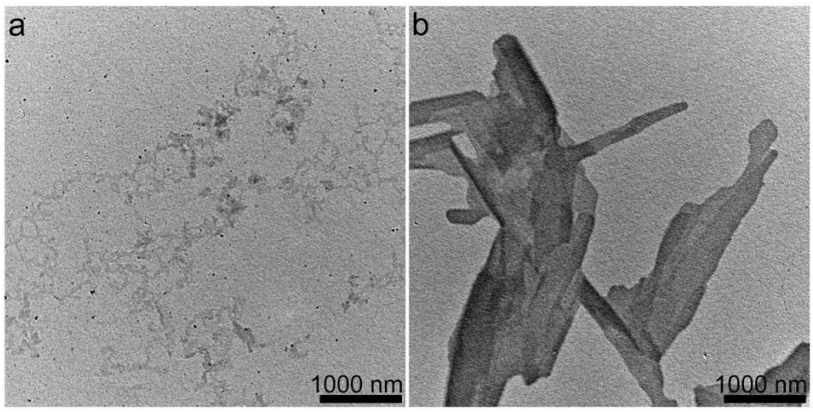

Figure S29. TEM images obtained by drop-casting an aliquot of solutions of (a) $[PCE][NO_3]_n$ in water and (b) $[Na][C_{16}$-L-Ala] in a mixture of water and ethanol (1:1 in volume ratio) drop cast onto carbon-coated copper grids.

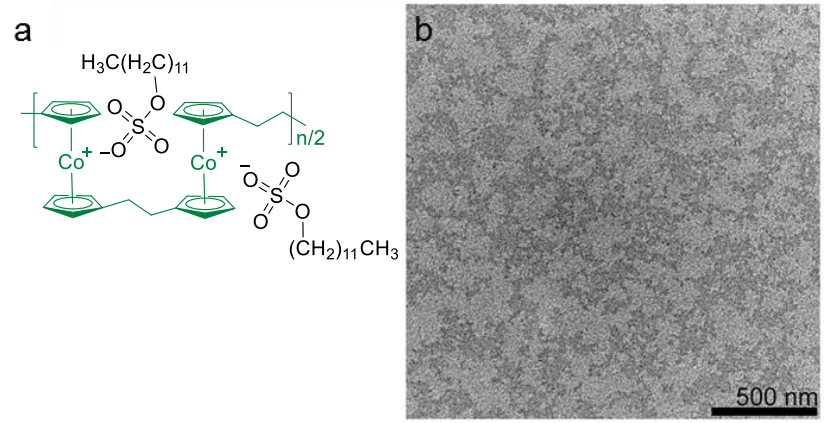

Figure S30. a) Molecular structure of $[PCE][SDS]_n$ and b) TEM image obtained by drop-casting an aliquot of solution of $[PCE][SDS]_n$ complex in ethanol on a carbon-coated copper grid.

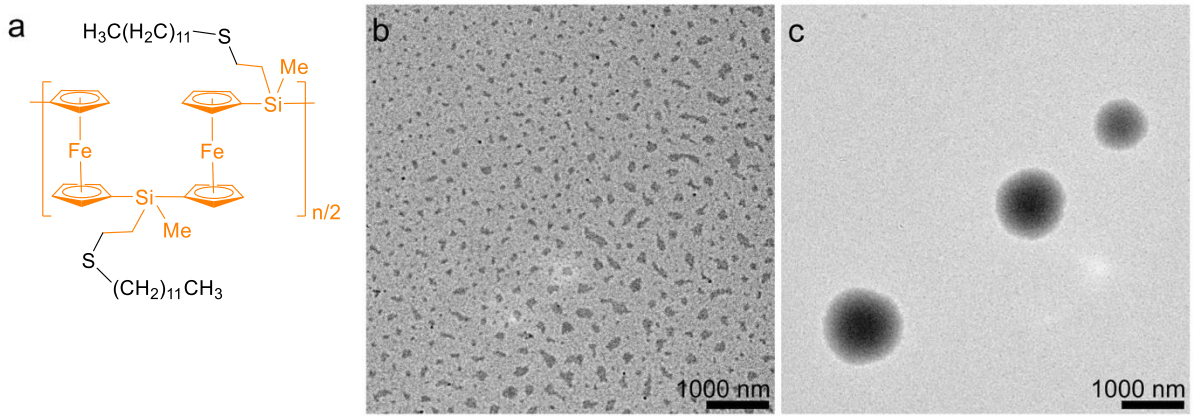

Figure S31. a) Molecular structure of PFS-C_{12} and TEM images obtained by drop-casting an aliquot of solutions of PFS-C_{12} in b) hexane and c) isopropanol on a carbon-coated copper grid.

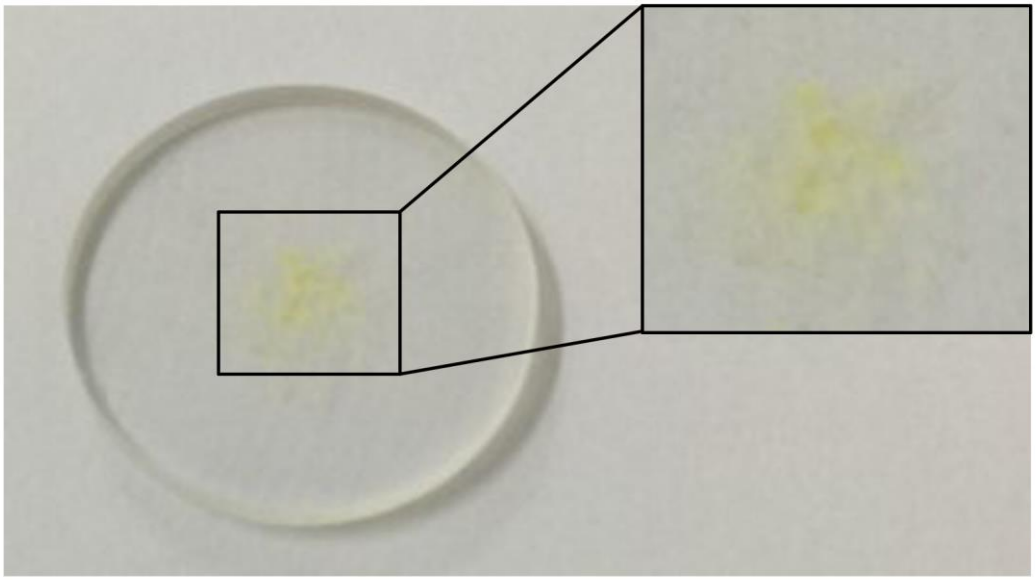

Figure S32. Photograph of yellow [PCE][C_{16}-L-Ala]$_n$ precipitate of helical assemblies (isolated after dialysis with water) pressed between two quartz plates during sample preparation for solid-state CD measurements.

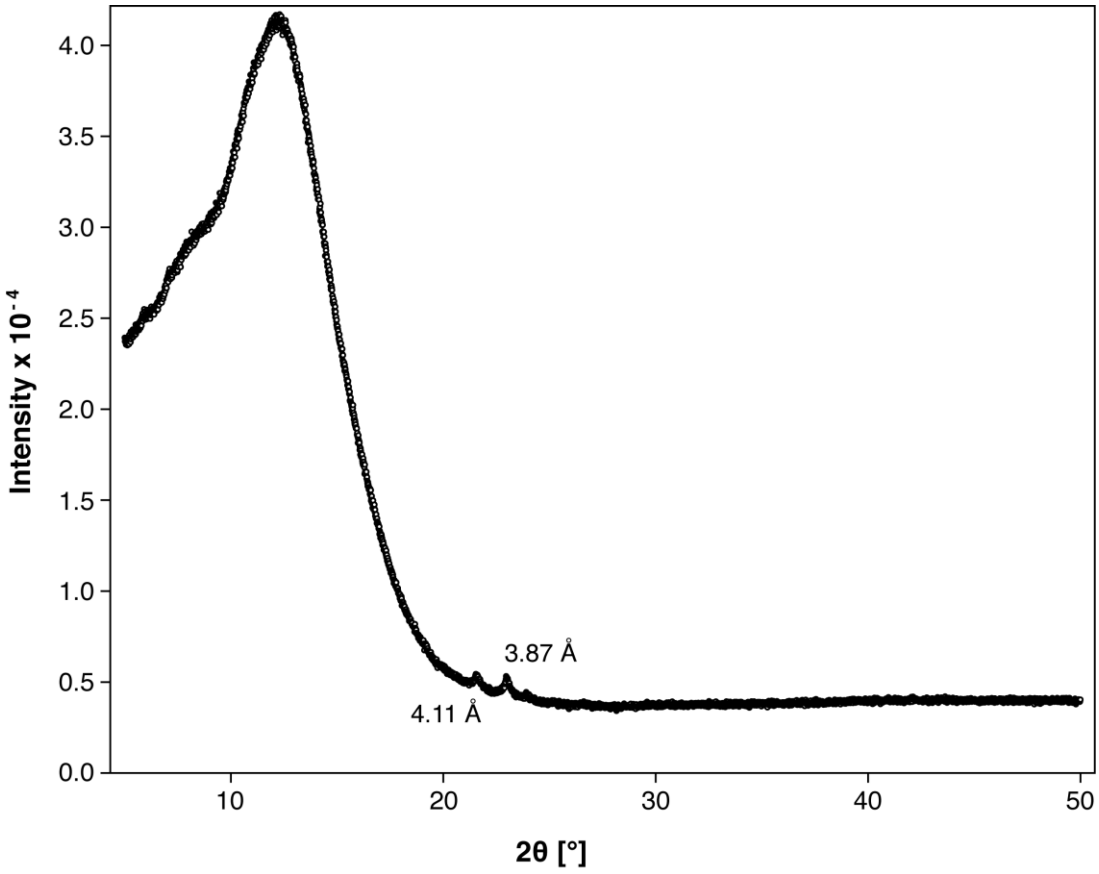

Figure S33. WAXS data for helical assemblies of [PCE][C_{16}-L-Ala]$_n$ from water.

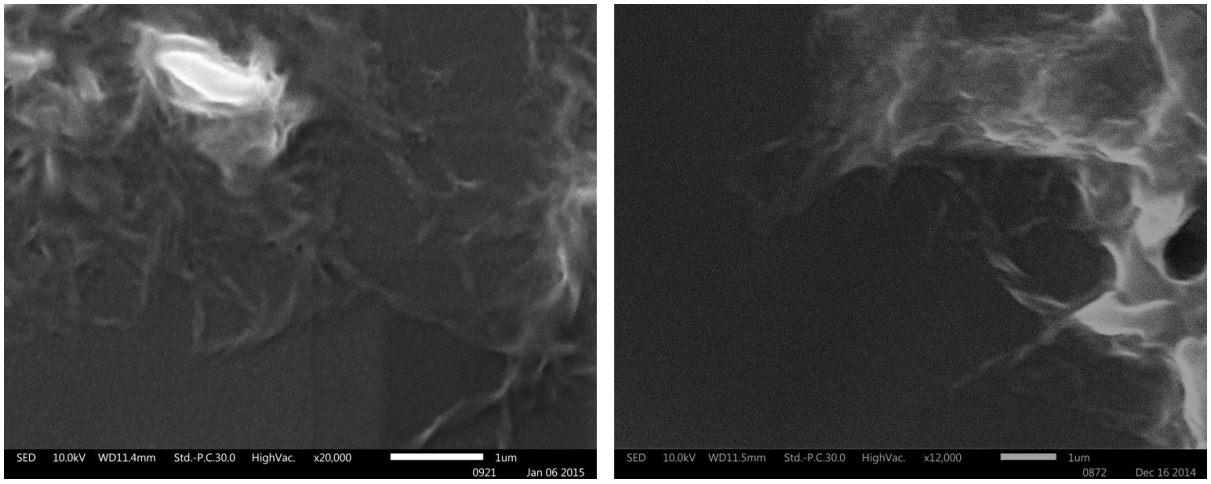

Figure S34. Additional representative SEM images of helical assemblies of [PCE][C_{16}-L-Ala]$_n$ in water onto a carbon-coated copper grid which has been sputter-coated with Pt/Pd alloy.

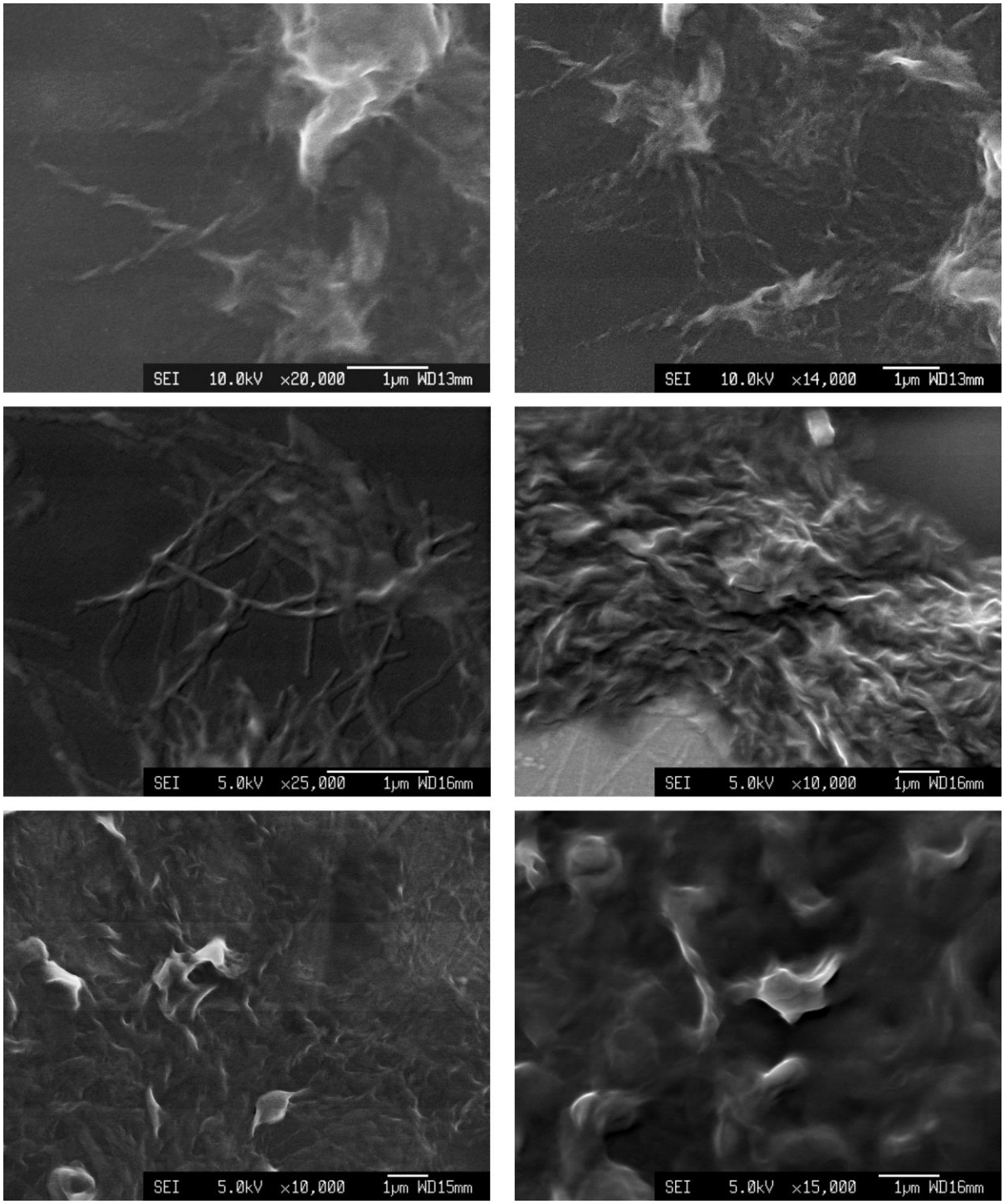

Figure S35. Additional representative field emission SEM (FE-SEM) images of assemblies of [PCE][C_{16}-L-Ala]$_n$ in water on a carbon-coated copper grid with subsequent sputter-coating with Pt/Pd alloy.

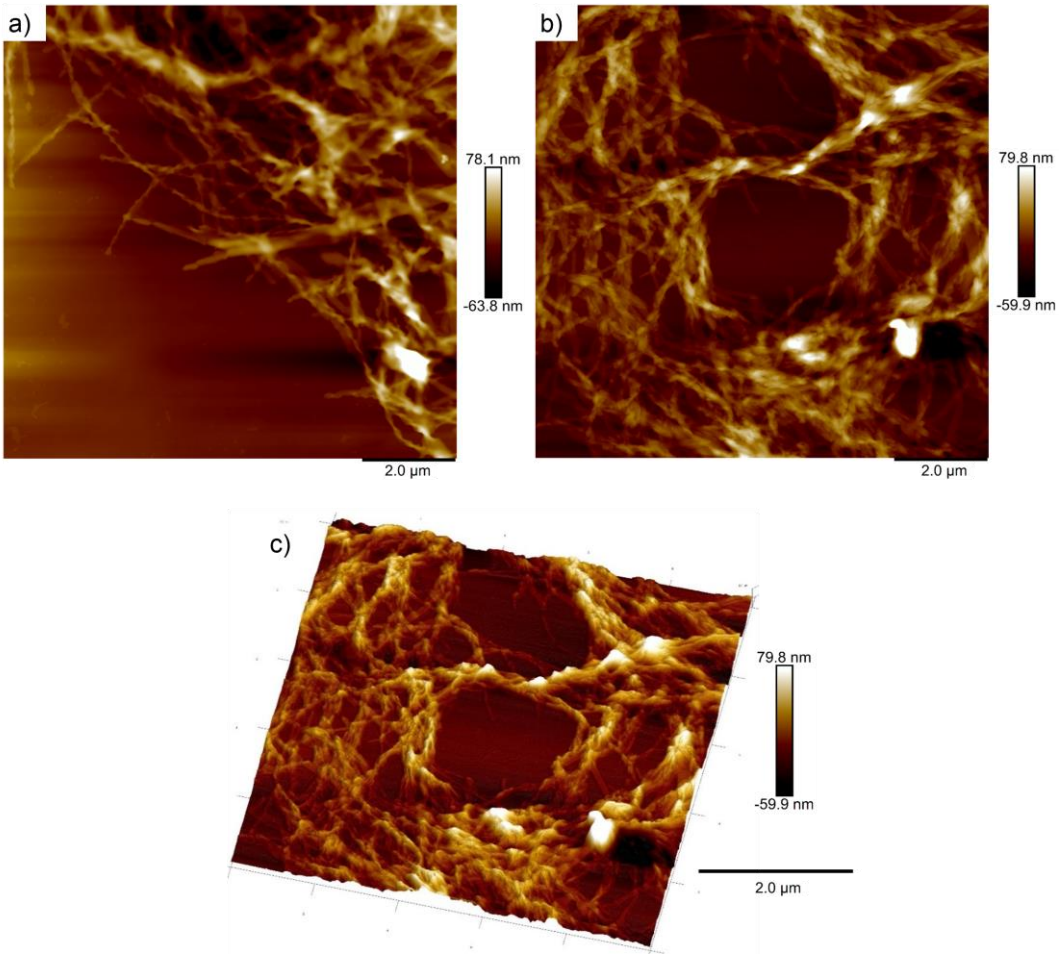

Figure S36. Additional AFM images obtained by drop-casting an aliquot of suspensions of [PCE][C_{16}-L-Ala]$_n$ in water onto a carbon-coated copper TEM grid

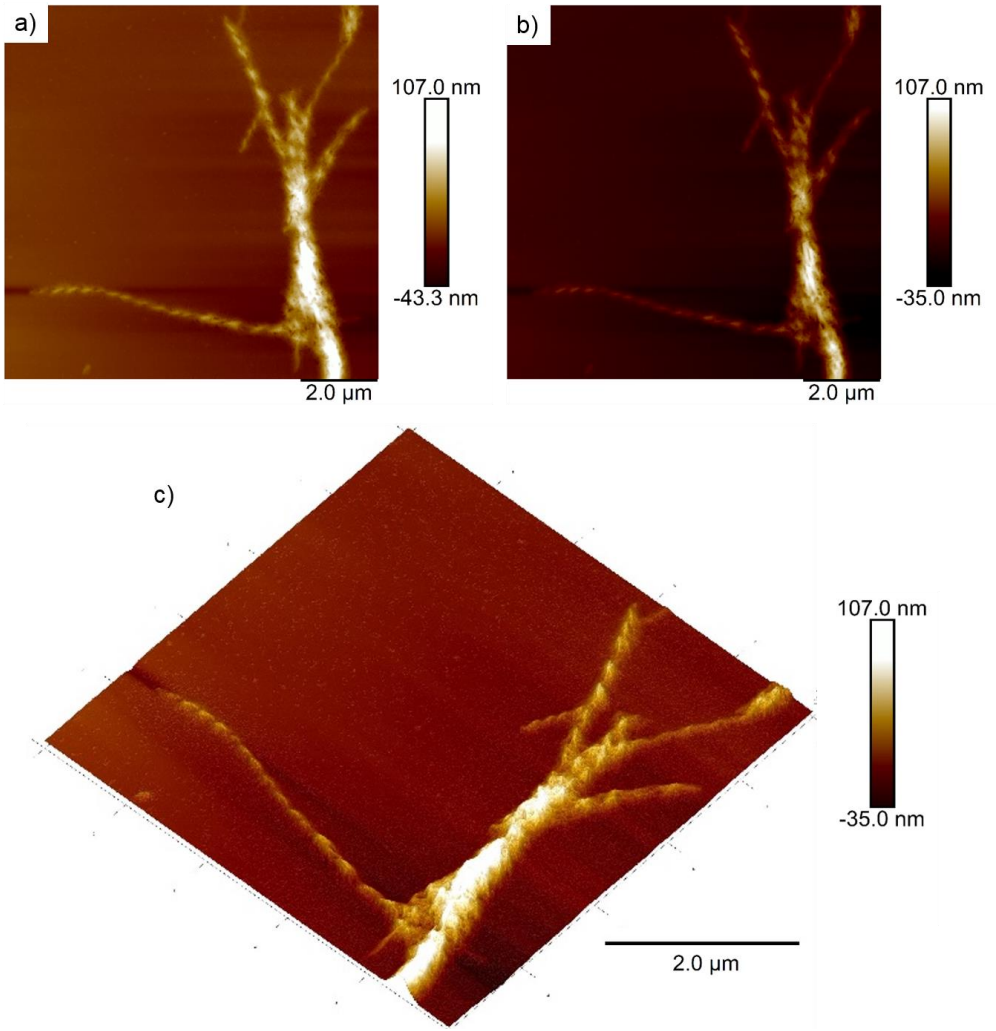

Figure S37. Additional AFM images obtained by drop-casting an aliquot of suspensions of [PCE][C_{16}-L-Ala]$_n$ in water onto a freshly cleaved mica surface.